WEMPEC

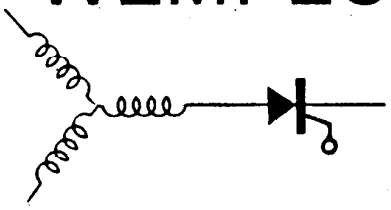

Wisconsin Electric Machines and Power Electronics Consortium

RESEARCH REPORT
82-6

Design and Control Techniques For Extending High Frequency Operation of a CSI Induction Motor Drive

T.A. Lipo
University of Wisconsin
Madison, Wisconsin

L.H. Walker
General Electric Company
Salem, Virginia

Department of Electrical and Computer Engineering
University of Wisconsin-Madison
Madison, Wisconsin 53706

June 1982

Design and Control Techniques for Extending High Frequency Operation of a CSI Induction Motor Drive

THOMAS A. LIPO, SENIOR MEMBER, IEEE, AND LOREN H. WALKER, SENIOR MEMBER, IEEE

Abstract—**An investigation of the maximum speed capability of a current source inverter (CSI) drive in both a three- and a six-phase connection is presented. It is shown that a six-phase configuration has distinct advantages over a three-phase connection in high speed capability for the same peak motor spike voltages. In addition, with proper control of the firing pulses fed to the inverters supplying the six-phase machine, the speed range can be substantially extended beyond the maximum limit predicted using conventional control. Predicted analytical results are correlated with results obtained by a detailed hybrid computer simulation.**

INTRODUCTION

THE PAST DECADE has witnessed the emergence of the current source inverter (CSI) induction motor drive in the high horsepower adjustable speed drive market. Since regeneration and reversing are inherent in a CSI drive, it has performance comparable to a fast reponse dc motor drive. A limiting factor in pushing up the horsepower rating of such drives to ever increasing sizes is the high peak voltages resulting from the rapid switching of inductive currents which flow due to the induction motor load. These voltages appear as quarter-cycle high frequency spikes which ride atop a nearly sinusoidal stator voltage waveform. These recurring voltage spikes necessitate the use of high voltage silicon-controlled rectifiers (SCR's) and diodes even when the fundamental component of the voltage waveform is relatively modest.

As one way to raise the horsepower limit, attention is turning to multiple groups of inverters directly feeding separate machine windings as shown in Fig. 1. It can be noted that the stator windings of the machine consist of a pair of three-phase groups mutually displaced by 30 electrical degrees. Such a winding configuration can be easily constructed by "splitting" the usual 60 deg phase belt into two portions each spanning 30 deg [1]. The machine can be viewed as having an asymmetric six-phase winding since the six resulting phases are not symmetrically displaced by 60 deg. An important advantage in an asymmetric connection over a symmetric one is that when such a stator winding arrangement

Paper IPCSD 83-19 is a revised version of a paper, approved by the Industrial Drives Committee of the IEEE Industry Applications Society for presentation at the 1982 Industry Applications Society Annual Meeting, San Francisco, CA, October 4-8. Manuscript released for publication March 10, 1983.

T. A. Lipo is with the Department of Electrical and Computer Engineering, University of Wisconsin-Madison, 1415 Johnson Drive, Madison, WI 53706.

L. H. Walker is with the Drive Systems Department, General Electric Company, 1501 Roanoke Boulevard, Salem, VA 24153.

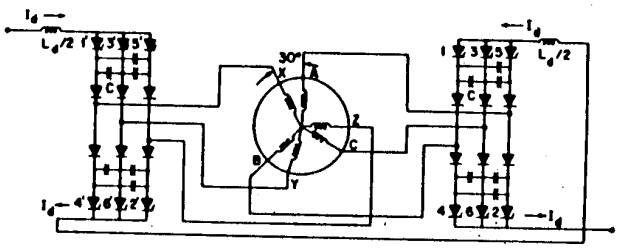

Fig. 1. Dual six-pulse current source inverter induction motor drive.

is fed from properly timed displaced six-pulse bridges, the lowest frequency torque pulsation becomes the twelfth rather than the sixth harmonic.

Another important limiting factor in extending the horsepower capability is the rather limited speed range resulting from commutation problems with the CSI inverter. In general, it is very desirable to increase the output frequency as much as possible since this often permits a reduction in size and cost of the associated motor. Even though the solid-state devices used in the inverter are capable of a very high switching frequency, the commutation interval for the inverter is relatively long, substantially greater than for a voltage source inverter of equivalent rating. These problems arise primarily because the commutating inductance, which together with the commutation capacitors form the resonant inductance-capacitance (*LC*) circuit, consists of the leakage inductances of the motor. The choice of this inductance is generally not under control of the inverter circuit designer. In addition, the counter electromotive force (EMF) of the motor appears in the commutation path which results in an additional delay in the transfer of current.

In this paper it is shown that the use of a six-phase system rather than a three-phase system permits a significant increase in the speed range that can be achieved before commutation problems arise. In addition, it is shown that by proper control of the two inverters, even higher speeds can be realized. The projected improvement in speed range is substantiated by a detailed hybrid computer simulation of the entire system.

COMMUTATION LIMIT FOR THREE-PHASE MACHINES

Studies of commutation of auto-sequentially-commutated (ASCI) type CSI inverters have been extensively published [2], [3]. In general, three modes of operation can be identified: single commutation, double commutation, and multiple commutation. During a single commutation, current transfers occur independently in either the top or bottom half of the bridge.

0093-9994/83/0900-0744$01.00

That is, only one commutation at a time occurs at any instant. The single commutation mode is in effect whenever the current transfer takes place within 60 electrical degrees and can be considered as the normal mode of operation.

When the commutation takes longer than 60 deg, a commutation is initiated in the top (bottom) half of the bridge before the commutation in the bottom (top) half has been completed. Double commutation takes place in which the dc link is temporarily shorted by series-conducting SCR's in the top and bottom halves of the bridge. When the commutation delay reaches 120 deg, the multiple commutation interval is entered in which the dc link and, consequentially, the motor is continuously short circuited. Control is abruptly lost because of the rotating short circuits. Since the machine is no longer able to sustain properly its reactive excitation current, an uncontrolled oscillation results. Hence, the 120 deg point represents the limiting case for practical operation.

It is of interest to determine analytically this critical point since it sets an upper limit on the speed range that can be achieved for a given set of system parameters. Calculation of the critical 120 deg point can be readily computed if it is assumed that commutation in the top and bottom of the bridge takes place independently. Although this assumption is correct during the single commutation interval it is not completely valid for the double commutation interval due to the possibility of additional charging [3]. However, it appears that this charging has only a small effect, if any, on the commutation time.

Consider, for example, a commutation from SCR 1 to 3 in Fig. 1. Fig. 2 shows the corresponding capacitor voltage and current which typically occurs during a commutation interval. The relevant capacitor during a commutation from SCR 1 to 3 is denoted as C in Fig. 1. Note that the capacitor is initially charged to a negative voltage $-V_c$. When the next oncoming thyristor is fired, the capacitor C is essentially placed in series with the dc link current and in parallel with the remaining two capacitors in the top half of the bridge. This results in a linear positively increasing voltage across the capacitor. The end of this interval occurs when the capacitor voltage exceeds the instantaneous motor line-to-line voltage across the two phases in which the capacitor is connected.

In general, maximum delay occurs when the charging time is greatest. That is, the delay t_1 in Fig. 2 is greatest when the current is a minimum, i.e., the no load condition. If the no load case is assumed then transfer begins to take place when $v_c = \sqrt{6}V_m$ where V_m is the root-mean-square (rms) value of the air gap voltage per phase. The delay time t_1 is expressed by [3]

$$t_1 = 2\sqrt{6}\frac{V_m C'}{I_d} + \sqrt{2L_s' C'} \tag{1}$$

where I_d is the dc link current, L_s' is the motor transient inductance per phase as viewed from the stator terminals, and C' is the effective capacitance prevailing during a commutation. That is

$$C' = \frac{3C}{2}.$$

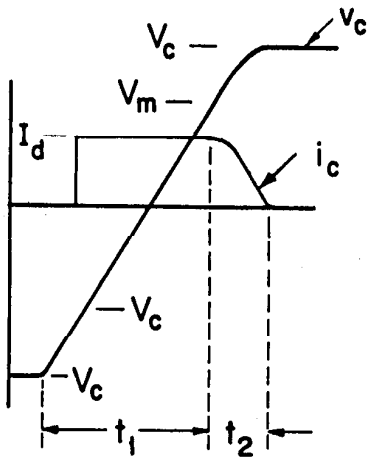

Fig. 2. Capacitor voltage and current commutation waveforms.

When the charging interval ends, the interval t_1 is followed by a quarter cycle ring in which the transfer of current from the offgoing to the ongoing diode is accomplished. The time required to complete the quarter cycle ring is

$$t_2 = \frac{\pi}{2\omega_0}$$

$$= \frac{\pi}{2}\sqrt{2L_s' C'}. \tag{2}$$

The quantity ω_0 is the resonant angular frequency of the LC circuit. The amplitude of the voltage spike produced by the quarter cycle ring which appears from line-to-line is

$$V_{spike} = I_d\sqrt{\frac{2L_s'}{C'}}. \tag{3}$$

The total commutation time is therefore expressed as

$$t_1 + t_2 = \frac{2\sqrt{6}V_m C'}{I_d} + \left(1 + \frac{\pi}{2}\right)\sqrt{2L_s' C'}. \tag{4}$$

The dc link current is related to the rms fundamental component of motor current by

$$I_d = \frac{\pi}{\sqrt{6}} I_1. \tag{5}$$

Although (5) is derived by assuming ideal rectangular ac currents, it remains reasonably accurate for finite link inductors.

If no load operation is assumed then (5) can be written as

$$I_d = \frac{\pi}{\sqrt{6}} I_{eb}\left[\frac{V_m}{V_b}\frac{\omega_b}{\omega_e}\right] \tag{6}$$

where I_{eb} is a base or reference value of excitation current, V_b and ω_b are the corresponding value of base voltage and base angular frequency, respectively, and ω_e is the actual motor angular frequency.

Equation (4) can now be written as

$$t_1 + t_2 = \frac{12}{\pi}\frac{C'V_b\omega_e}{I_{eb}\omega_b} + \left(1+\frac{\pi}{2}\right)\sqrt{2L_s'C'}. \tag{7}$$

When commutation time requires 120 electrical degrees then

$$t_1 + t_2 = \frac{2\pi}{3\omega_e}. \tag{8}$$

If we set (7) equal to (8) it can be shown that the following quadratic equation results

$$\omega_e^2 + \left[\frac{\pi(2+\pi)}{24}(\sqrt{2L_s'C})\frac{I_{eb}\omega_b}{C'V_b}\right]\omega_e + \frac{\pi^2}{18}\frac{I_{eb}\omega_b}{C'V_b} = 0. \tag{9}$$

The roots of (9) are the critical frequencies at which 120 deg overlap occurs and are expressed by

$$\omega_c = -\frac{\pi(2+\pi)}{48}\frac{K}{\omega_0} \pm \sqrt{\left[\frac{\pi(2+\pi)}{48}\right]^2\left(\frac{K}{\omega_0}\right)^2 + \frac{\pi^2}{18}K} \tag{10}$$

where

$$K = \frac{I_{eb}\omega_b}{C'V_b}$$

$$\omega_0 = \frac{1}{\sqrt{2L_s'C'}}.$$

Since the critical frequency must be positive, only the positive value of the square root term is relevant.

Equation (10) can be expressed in a different form if it is recalled that the ratio of rated air gap volts per hertz to excitation current is simply the air gap mutual inductance, i.e.,

$$\frac{V_b/\omega_b}{I_{eb}} = L_m. \tag{11}$$

Hence (10) becomes

$$\omega_c = -\frac{\pi(2+\pi)}{48}\frac{1}{L_m}\sqrt{\frac{2L_s'}{C'}} + \sqrt{\left[\frac{\pi(2+\pi)}{48}\right]^2\left(\frac{2L_s'}{L_m^2C'}\right) + \frac{\pi^2}{18}\left(\frac{1}{L_mC'}\right)} \tag{12}$$

TABLE I
PARAMETERS FOR THREE-PHASE SYSTEM

Machine Rating	Machine Parameters		Inverter and Link Parameters	
920 hp	r_s	= 0.0035 Ω	C	= 767 μF
3 phase	X_{ls}	= 0.0110 Ω	L_d	= 2.8 mH
460 V	r_r'	= 0.0019 Ω		
6 poles	X_{lr}'	= 0.0065 Ω		
45 Hz	X_m	= 0.4310 Ω		

which can be rearranged to the form

$$\frac{\omega_c}{\omega_0} = \frac{\pi(2+\pi)}{24}\left[-\frac{L_s'}{L_m} + \sqrt{\left(\frac{L_s'}{L_m}\right)^2 + \frac{64}{(2+\pi)^2}\left(\frac{L_s'}{L_m}\right)}\right]. \tag{13}$$

Equation (13) demonstrates that the critical frequency can be considered as a property of the machine and is related to the ratio of motor transient reactance to magnetizing reactance. The critical frequency is clearly increased by a decrease in the commutating capacitance C. However, this increase is accomplished only by a proportionate increase in the voltage spike (3) and becomes impractical due to device limitations. In as much as lowering L_s' allows a smaller C, reducing L_s' is advantageous.

Note from (13), however, that the critical frequency can also be increased by an appropriate reduction in the magnetizing inductance L_m. Unfortunately, the voltage spike again increases because of the increased magnetizing current. Once both L_m and L_s' have been reduced to their practical limit, further extension of high speed operation can only be achieved by control methods.

In order to verify the validity of the results developed thus far, a detailed simulation of an actual breadboard was implemented on a hybrid computer. In particular, current source inverter was modeled in complete detail with an accurate representation of all six diodes, SCR's, and capacitors in the inverter [5]. The system parameters used for this study are summarized in Table I. The capacitor values of 767 μF were chosen so as to limit the voltage spike to 670 V.

The details of the motor control system are clearly beyond the scope of this paper. However, the control functions which were used were identical to the system described in an earlier paper and have been implemented in hardware [8]. Substitution of the parameters of Table I into (10) indicates that the predicted critical frequency is 78 Hz.

For purposes of comparison Fig. 3 shows a computer recording in which the motor is operating under the no load condition at base frequency (45 Hz). In this figure and all subsequent computer traces, the time axis proceeds horizontally from left to right. Note the classical waveforms developed across the inverter devices particularly across the capacitor [3]. The commutation time can be identified by the time required for the capacitor to ramp from its positive

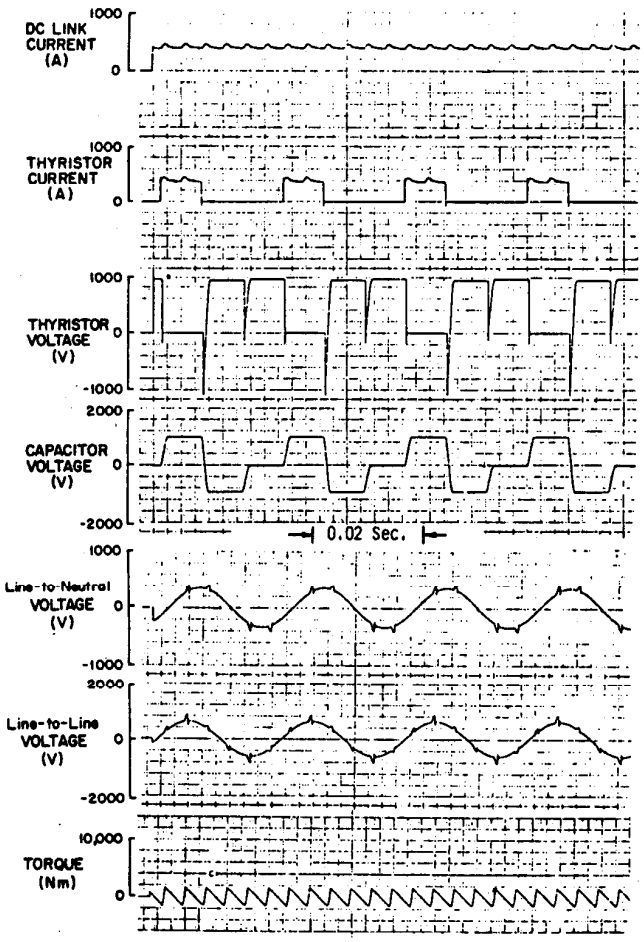

Fig. 3. Operation of three-phase machine with six-pulse bridge at no load and at base frequency (45 Hz).

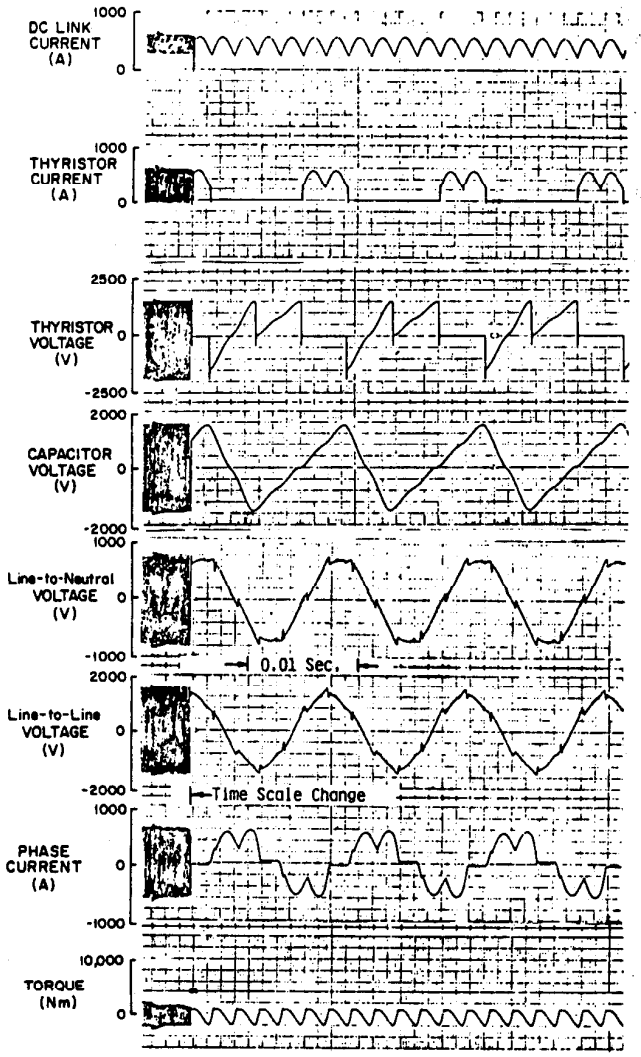

Fig. 4. Operation of three-phase machine with six-pulse bridge at no load. Step change in frequency from 80 to 85 Hz.

to its negative value (approximately 17 deg in Fig. 3). Fig. 4 shows a computer trace of the machine operating at the critical frequency. It is apparent that the commutation time has increased markedly. In particular, it can be noted that the capacitor voltage has assumed a triangularlike waveshape in which the "dwell time" or intervals of constant capacitor voltage have essentially been eliminated. Hence, the inverter is continually in the process of commutation, and the 120 deg overlap has been reached as predicted.

Although the critical frequency is reached at 78 Hz, the computer simulation indicates that stable operation can be maintained to somewhat higher value. Simulation studies on this system indicate that instability will actually occur somewhere between 85 and 90 Hz. Fig. 5 is a computer trace showing the transient behavior of the system as the inverter frequency is suddenly changed from 85 to 90 Hz. It can be observed that the system breaks into an uncontrolled oscillation. The high harmonic content in the stator current can be noted as well as in the motor voltages which have now become quite nonsinusoidal. The waveforms obtained at both critical frequency and slightly above critical correlate well with previously published test results in [3, Fig. 9]. The possible operation of the system slightly into the multiple commutation mode has also been experimentally observed in [3].

SIX-PHASE OPERATION

In many cases the upper frequency limit, 80–85 Hz in the system under investigation, severely limits the available speed range of a current source drive. One possible means for extending high frequency operation is to rewind the machine in six-phase fashion. In essense, each three-phase winding is separated into two distinct groups which are phase shifted by 30 electrical degrees. The resulting adjustments in machine parameters is best illustrated by first considering a simple inductor, illustrated in Fig. 6, in which two components can be identified, a magnetizing or useful component which typically would flow in an iron core and a leakage or stray component for which the path of the flux lines close in air. It is clear that such separation is purely artificial for the case of a simple inductor but is useful conceptually when extended to an ac machine.

If the winding making up the inductor is separated into two equal parts, the resistance of each group becomes one-half the original resistance while the inductances change by a factor of four since the number of turns of each winding

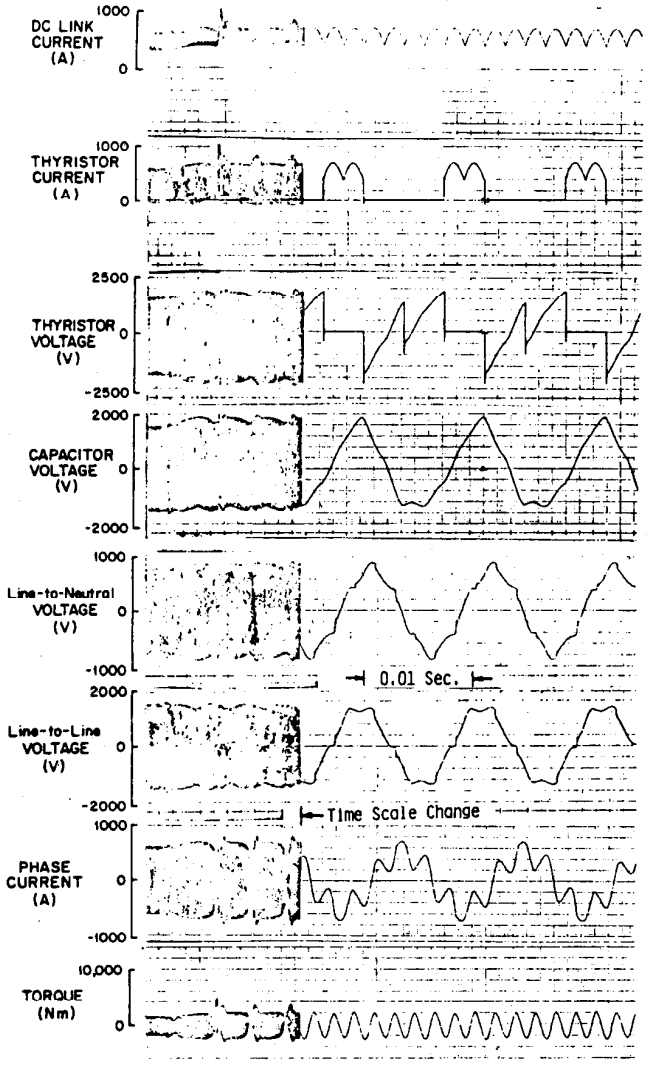

Fig. 5. Operation of three-phase machine with six-pulse bridge at no load. Step change in frequency from 85 to 90 Hz.

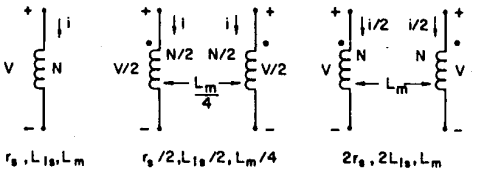

Fig. 6. Conceptual modification of single winding reactor to dual windings having the same voltage ratings.

has been halved. In addition, a mutual coupling is introduced since the original winding was wound around a single magnetic core. This inductance is also proportional to one-fourth the original magnetizing reactance since the "primary" and "secondary" windings have the same number of turns.

Since each winding has $N/2$ turns it is capable of supporting one-half the original voltage. In practice however, it may be desirable that each winding supports the total rated voltage rather than one-half this value. This can be accomplished by a simple rewind in which the number of turns is doubled in each of the two groups from $N/2$ to N while the cross sectional area of the winding is halved so that the total copper

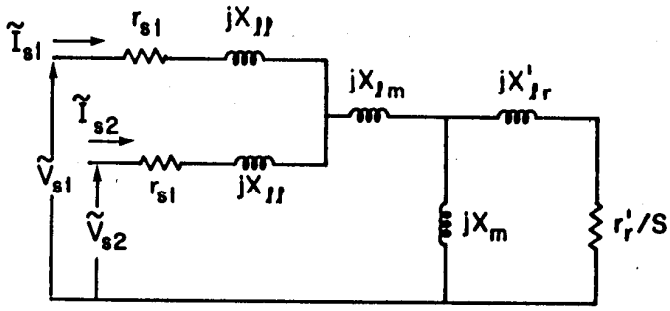

Fig. 7. Phase steady state equivalent circuit of asymmetric six-phase induction motor.

cross sectional area remains the same. The resulting leakage and magnetizing inductance become equal to the original values while the resistance of each winding becomes twice the original value. A pictorial illustration of this reasoning process is given in Fig. 6. It should be emphasized that extension of this reasoning process to a six-phase induction machine is considerably more complicated. Proper attention must be paid to changes in winding factors as well as the effects of belt and zigzag leakage inductances, none of which is present in the simple example of Fig. 6.

This conceptual picture can be extended to ac machine design. However, the parameters which result are not so readily calculated for several reasons. First, the two "split" windings are now physically located in slots so that their magnetic axes are not aligned but displaced by 30 deg. Secondly, the separation of the windings into two portions changes their pitch and distribution factors so that the fundamental number of turns is modified. This modification in the effective turns increases somewhat the value of magnetizing inductance. Thirdly, the windings are now coupled to a secondary, namely the rotor windings. The change in the fundamental components of primary pitch and distribution factors results in different values of secondary leakage inductance and resistance when referred to the stator. Finally, the separation of the windings into the groups introduces a mutual coupling between the groups which involves only flux lines which were originally associated with leakage flux. This term arises for reasons similar to the case of the simple inductor of Fig. 6. A modified steady state per phase equivalent circuit which accounts for this extra coupling is shown in Fig. 7.

Table II gives a comparison of the parameters for the original three-phase machine and the redesigned six-phase machine, respectively. Note that all parameters of the redesigned machine are different even though the three-phase windings have been essentially split in half. An extra parameter X_{lm} has been introduced to account for the coupling due to slot leakage flux. A detailed discussion of the design and modeling of this machine is given in [6].

If it is again assumed that the commutating inductance is essentially given by the sum of the primary and secondary leakage inductances, the required capacitance for the same 670 V spike can again be calculated by use of (3). In this case $C = 233\ \mu F$ which is about 30 percent the value required for the three-phase case. Twelve rather than six capacitors are needed for this connection. However, the installed kVA-s

TABLE II
PARAMETERS OF SIX-PHASE SYSTEM

Machine Ratings	Machine Parameters		Inverter and dc Link Parameters	
920 hp	r_{s1}	= 0.0070 Ω	C	= 233 μF
6 phase	X_{ll}	= 0.00728 Ω	L_d	= 2.8 mH
460 V	X_{lm}	= 0.00768 Ω		
6 poles	r_r	= 0.00204 Ω		
45 Hz	X_{lr}'	= 0.00697 Ω		
	X_m	= 0.4620 Ω		

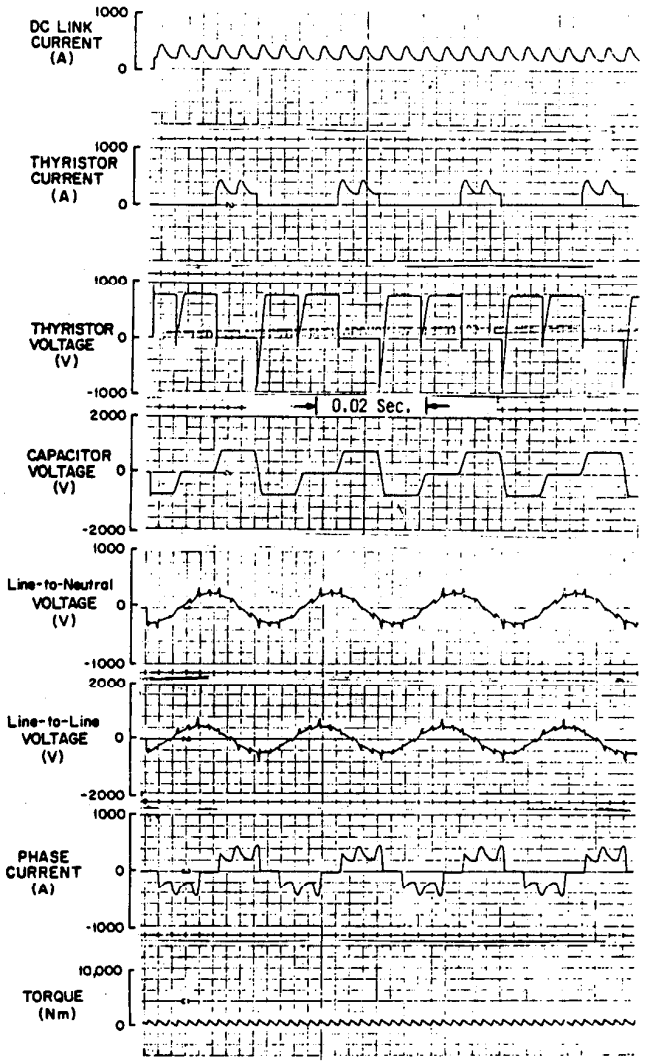

Fig. 8. Operation of six-phase machine with dual six-pulse bridges at no load and at base frequency (45 Hz).

capacity need be only 60 percent of the value required for the three-phase connection. The corresponding critical frequency for six-phase operation can be obtained by use of (13) and becomes 100 Hz, a 28 percent improvement in speed range and, effectively, horsepower capability of a properly designed motor.

Fig. 8 again shows, for reference purposes, the behavior of the six-phase machine when driven from a dual inverter supply at base frequency. The solution was again obtained from a detailed model of both motor and inverters. The simulation of the six-phase motor is described in detail in [6]. Simulation of the inverter again uses [5]. Again no load motor operation is assumed. It is interesting to compare the torque pulsations which occur under this condition compared to the three-phase case (Fig. 3). Note that the frequency has been doubled while the amplitude has been halved in accordance with theory. Twelve spikes rather than the usual six per cycle can be located on the motor line-to-line and line-to-neutral voltages.

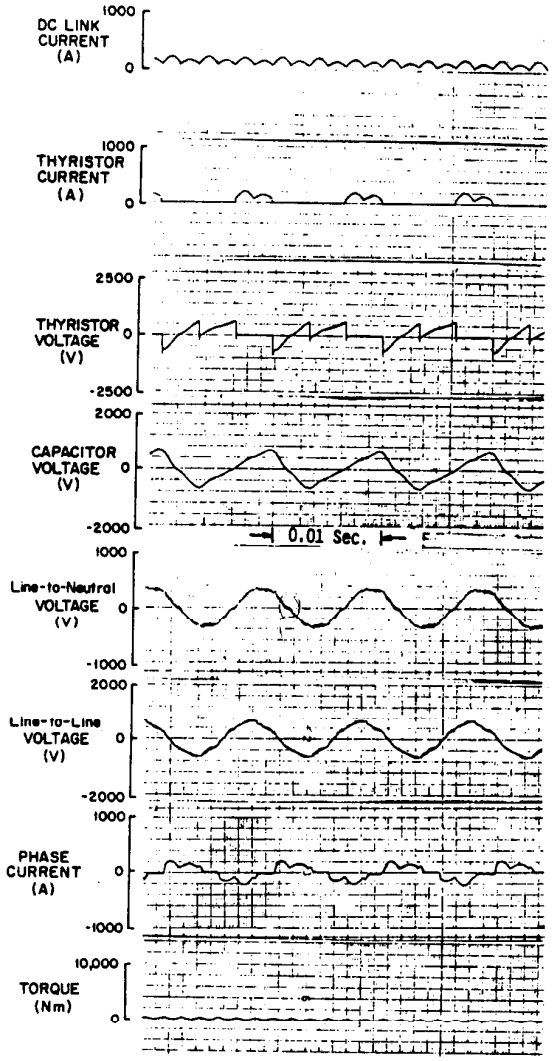

Fig. 9. Operation of six-phase machine with two six-pulse bridges at 100 Hz with no load.

Fig. 9 shows the operation of the motor at the 100 Hz critical frequency point in which the commutation time is predicted to require 120 deg. Examination of the capacitor voltage again verifies that the 120 deg commutation point has been reached. Hence, (10) derived originally for three-phase machines appears to be equally valid if the machine is wound with a six-phase connection. Again, operation slightly beyond this point appears possible. The limiting frequency of operation for the system with the parameters chosen appears to be in the vicinity of 120 Hz. Fig. 10 illustrates the behavior of the system when the inverter frequencies are step changed

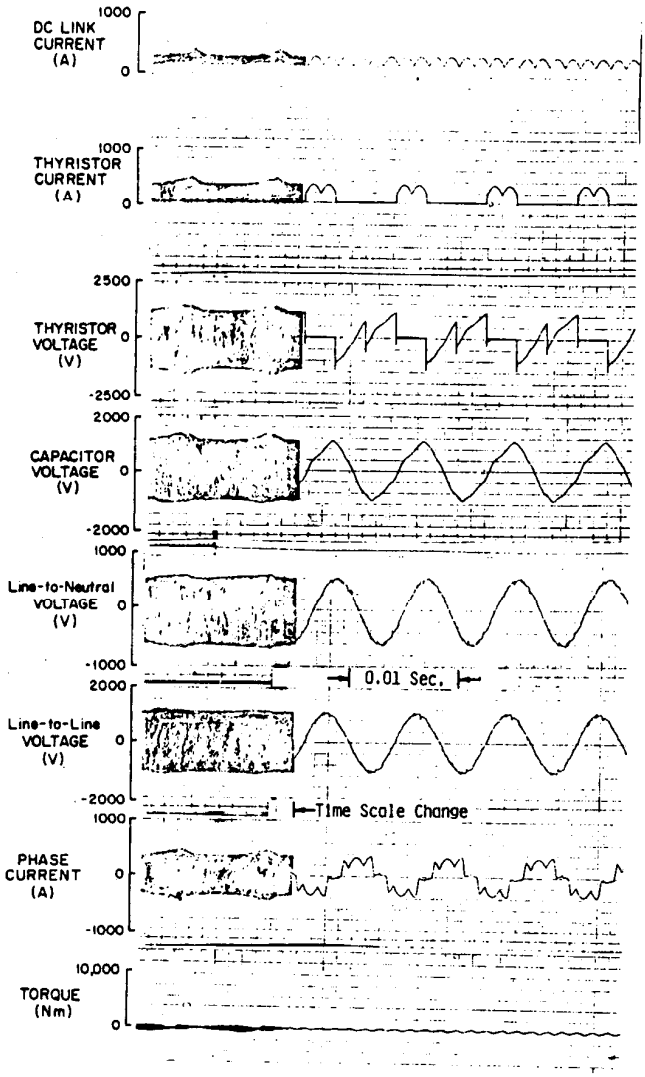

Fig. 10. Six-phase induction machine with dual converters. Step change in frequency from 115 to 120 Hz.

from 115 to 120 Hz. Note that the system again breaks into oscillation.

CONTRASHIFT CONTROL METHOD

It should now be apparent that substantial benefits can be derived by utilizing six-phase rather than three-phase current fed machines. In particular approximately a 30 percent increase in speed range appears possible with a six-phase machine with the same frame size. Further improvements, however, appear to be limited by the same geometric constraints as the three-phase machine, namely the constraints implied by (13). However, examination of another form for the critical frequency, namely (10), suggests a means by which the critical frequency can be extended still further. Note that the factor K contains the ratio of the base excitation current to base volts per hertz. If the base excitation current could in some manner be allowed to increase without altering the base volts per hertz, the critical frequency could be correspondingly increased. This desirable increase in excitation current can, in fact, be accomplished by phase shifting the two bridges

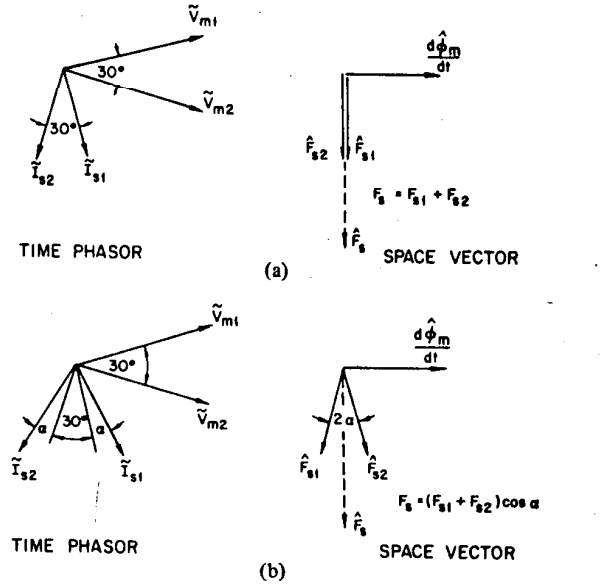

Fig. 11. Phasor and vector diagrams illustrating principles of contrashift. (a) Without contrashift. (b) With contrashift.

appropriately. The technique employed to produce this effect is termed contrashift in order to emphasize the contrarotating phase shifts employed in the two inverters.

The principle of contrashift can be illustrated by reference to Fig. 11. In general, it can be recalled that the six-phase induction machine is wound with a pair of three-phase groups, mutually displaced by 30 electrical degrees. Uniform rotation of stator magnetomotive force (MMF) (current commutation waveforms (CCW) in Fig. 1) is obtained by phase shifting the spatially lagging phases in the machine (a, b, and c in Fig. 1) by a corresponding 30 deg in time, thereby making the fundamental components of the MMF's produced by the two three-phase groups rotate colinearly. A pictorial representation of the time phasors and space vectors for no load operation is shown in Fig. 11(a). At no load the air gap flux which links the windings is proportional to the net rotating MMF vector F_s within the machine. Consider now, the effect of advancing the firing of the x, y, z three-phase group while retarding the firing of the a, b, c three-phase group by a like amount. If it is assumed that the net MMF producing flux within the machine is unchanged then the two stator currents must increase in amplitude to the value $I_s/\cos\alpha$ in order to compensate for the fact that the two MMF's are not in phase. For example, when $\alpha = 30$ deg the currents in the two three-phase groups must increase by $2(I_s)/\sqrt{3}$ or $1.157*I_s$. Since the current in both groups increases by the same amount, the effect is readily accomplished by a 15 percent increase in the dc link current.

If the voltage across the phases is increased in a like proportion it is clear that no benefit could be derived since the ratio K in (10) would remain constant. However, the voltage induced in any winding is a function only of the net or resultant flux which is produced by the MMF F_s in Fig. 11(b) which has remained unchanged. Hence, the voltage remains constant for any contrashift angle α so that the contrashift angle can be advanced to almost arbitrarily high values limited

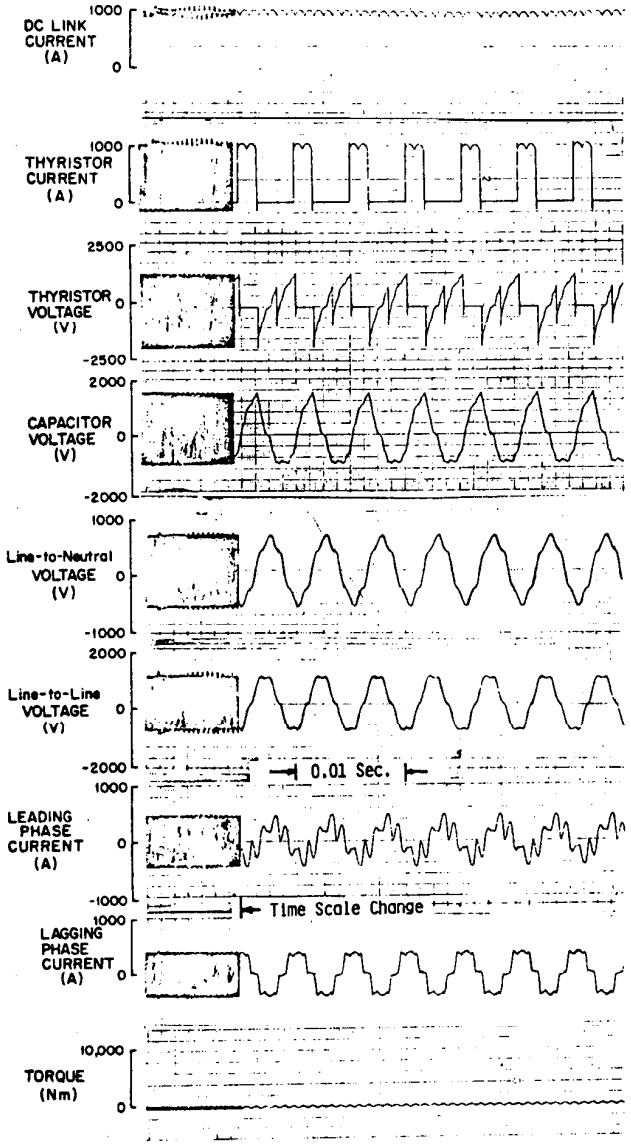

Fig. 12. Operation of six-phase machine with two six-pulse bridges phase shifted by ±30°. Step change in frequency from 190 to 195 Hz.

primarily by the increased losses in the inverter and motor which result from the increased dc link current.

Since the increase in dc link current for a contrashift angle of 30 deg is approximately 16 percent, examination of (10) would indicate that an extended speed range of approximately 8 percent would result. In practice, however, the speed range that can be realized is considerably larger. Fig. 12 is a computer trace which shows operation over the frequency range of 190 to 195 Hz when the contrashift angle has been set at 30 deg with the dc link current adjusted correspondingly to produce rated flux. Note, that the six-phase motor operates in stable fashion at 190 Hz and when the frequency is step changed to 195 Hz a very slight oscillation begins to take place. These oscillations become increasingly severe if operation beyond 195 Hz is attempted.

Successful operation to 195 Hz is certainly surprising and since it is more that 87 percent greater than the value predicted by theory, clearly some other effect is becoming dominant. With proper consideration of what is being achieved by contrashift, a satisfactory explanation of this phenomenon is possible. It can be recalled that throughout this study we have concerned ourselves with no load operation since it is well known that the 120 deg overlap condition occurs at no load earliest as frequency is increased [3]. The critical overlap condition slowly begins to envelop the motoring quadrant for increasingly larger values of motoring torque as frequency continues to increase [7]. The generating mode of operation, on the other hand, remains below the 120 deg overlap condition until the operating frequency becomes exceedingly large [7]. Examination of the phasor diagram, Fig. 11(b), verifies that while the motor is operating at no load, one of the two bridges is being advanced into the generating mode of operation while the other bridge is being retarded into the motoring mode. Hence, neither of the two bridges operates at no load, and the possibility of increasing the speed range by keeping both bridges out of the 120 deg overlap conditon becomes apparent. In practice, the motoring bridge reaches the 120 deg overlap first, but the overall system remains stable since control continues to be maintained through the generating bridge. Only when the generating bridge reaches its critical frequency does the overall system become unstable. Larger speed ranges appear possible with appropriate adjustment of the contrashift angle α.

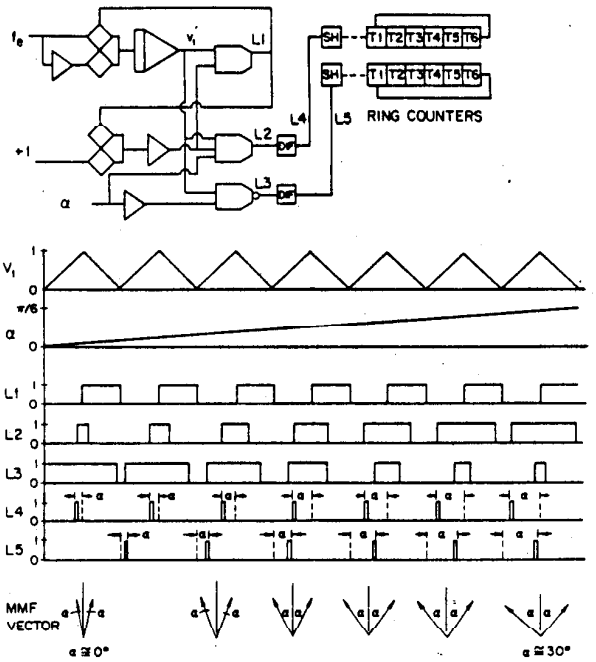

Fig. 13. Mechanization of contrashift angles in voltage controlled oscillator.

IMPLEMENTATION OF THE CONTRASHIFT PRINCIPLE

Fig. 13 gives a mechanization of a scheme which will produce a variable contrashift angle between 0 and 30 deg. Ring counter $T1$, $T2$, ···, $T6$ is used to fire the right-hand bridge of Fig. 1 while ring counter $T1'$, $T2'$, ···, $T6'$ is used to fire the left-hand bridge. The input to the circuit is an analog signal proportional to the inverter output frequency. Transi-

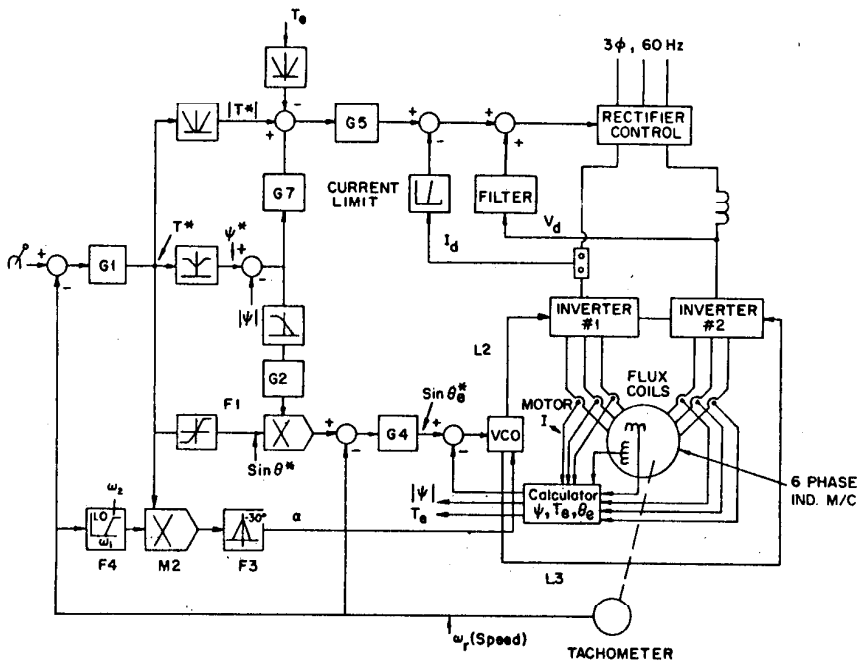

Fig. 14. Modified control system incorporating use of contrashift.

tions from a positive going to a negative going slope of an analog triangular wave are used to drive a ring counter which sets the firing signals for the right-hand bridge of Fig. 1. Transitions from a negative to a positive going slope drives another ring counter to set the firing pulses for the left-hand bridge. The angle α is introduced to produce the desired phase shift. Fig. 13 shows how the firing signals change as α is slowly increased from 0 to 30 deg. Modifications of this basic scheme for angles greater than 30 deg are readily derived.

Fig. 14 shows how the angle modulation scheme is implemented in a control scheme. The blocks in this control system are identical to a previously published scheme except for the addition of function generators $F3$ and $F4$, a multiplier $M2$, a modified voltage-controlled oscillator (VCO), and a modified "calculator." The remaining functional blocks are discussed at length in [8]. The purpose of function generator $F3$ is to increase the contrashift angle α in response to a speed error (i.e., a torque command). When the torque command is zero the contrashift angle is a maximum, taken arbitrarily to be 30 deg in this figure. The purpose of the function generator $F4$ is to begin increasing the contrashift angle at some predetermined speed denoted in Fig. 12 as ω_1. Below ω_1 the output of the function block $F4$ and also the multiplier $M2$ is zero so that the contrashift angle α is zero. When the speed reaches ω_2 the contrashift angle is completed in the circuit. The output of $F4$ is unity, and the multiplier output delivers the error signal of block $G1$ to the input of $F3$. The multiplier $M2$ serves to vary the gain of the input to $F3$ (the speed error) from zero to unity when the speed reaches a certain set point value ω_1. The gain reaches a maximum above ω_2. The modified VCO consists of the circuit in Fig. 13. The logic signals $L2$ and $L3$ on this figure have also been identified by $L2$ and $L3$ in Fig. 13.

The modified "calculator" of concern is that which senses the instantaneous angle between the MMF resulting from stator current and the air gap flux. The calculations performed are as described in [8] with the exception that the calculation for angle θ_e, as given by expression [8, (3)] must be performed separately for the two three-phase windings. The average of these two angle values is the actual angle used for comparison to the angle command, sin θ_e, in Fig. 14.

CONCLUSION

Continuing advancement in state-of-the-art converter design will undoubtedly lead to higher and higher horsepower applications. This paper has demonstrated that with present day device limitations, these high horsepowers are best accomplished by use of a multiple number of six-pulse converters fed to a machine equipped with isolated sets of three-phase windings. Although this paper has been concerned primarily with an asymmetric six-phase machine, it is clear that the approach is readily extended to machines having nine, twelve, or even more phases. In addition, unequal contrashift angles in the three-phase groups appear to be practical. Applications to even higher horsepower ranges would be possible by supplying only a fraction of the total motor pole pairs from a separate converter.

This paper has demonstrated that the use of an asymmetric six-phase connection permits an extension in the feasible speed range by 28 percent for the system studied without altering the copper and iron content in the machine. At the same time the use of a six-phase machine allows a 40 percent decrease in the size of the capacitors used to commutate the control of the two six-pulse bridges, the possible speed range can be extended by nearly a factor of two. This increase in range has been accomplished with only a modest increase in motor losses.

ACKNOWLEDGMENT

The authors wish to thank the General Electric Company for permission to publish this paper.

REFERENCES

[1] R. H. Nelson and P. C. Krause, "Induction machine analysis for arbitrary displacements between multiple winding sets," *IEEE Trans. on Power App. Syst.*, vol. PAS-93, May/June 1974.

[2] H. Kazuno, "Commutation of a three-phase thyristor bridge with commutation capacitors and series diodes," *Elec. Eng. Japan*, vol. 90, no. 5, pp. 91–100, 1970.

[3] W. Lienau, "Commutation modes of a current-source inverter," presented at Second IFAC Symposium Control Power Electron. Elec. Drives, Dusseldorf, W. Germany, 1977, pp. 219–229.

[4] W. Farrer and J. D. Miskin, "Quasi-sine-wave fully regenerative inverter," in *Proc. IEE (London)*, vol. 120, Sept. 1973, pp. 969–976.

[5] T. A. Lipo, "Hybrid computer simulation of an ASCI current source inverter," *Elec. Machines Electromechanics*, vol. 8, no. 1, pp. 1–15, Jan/Feb 1983.

[6] ——, "A d–q model for six phase induction machines," presented at International Conf. Elec. Machines, Athens, Sept. 15–17, 1980, pp. 860–867.

[7] W. McMurray, "The performance of a single-phase current fed inverter with counter EMF—Induction load," presented at IEEE Ind. Appl. Society Inter. Static Power Converter Conf., Mar. 28–31, 1977, pp. 483–496.

[8] L. H. Walker and P. M. Espelage, "A high performance controlled current inverter drive," *IEEE Trans. Ind. Appl.*, vol. IA-16, pp. 193–202, Mar./Apr. 1980.

Thomas A. Lipo (M'64–SM'71), for a photograph and biography please see page 553 of the July/August 1983 issue of this TRANSACTIONS.

Loren H. Walker (M'59–SM'78) received the B.E.E. degree from the University of Florida, Gainesville, in 1958, and the S.M. degree from the Massachusetts Institute of Technology, Cambridge, in 1961.

He first joined the General Electric Company in 1958. From 1958 to 1969 he developed inverters and cycloconverters for military and aircraft applications. From 1970 to 1972 he worked for the Exide Power Systems Division of ESB Inc., Raleigh, NC, developing large uninterruptible power supplies. He rejoined General Electric in 1972 at the Corporate Research and Development Center, Schenectady, NY, where he worked on a wide range of solid state power conversion applications. Since 1976 he has been with the Drive Systems Department of General Electric at Salem, VA. His primary work at this location has been in the development of variable frequency drives for large ac motors. He holds 39 US patents.